Energy Efficiency Maximization in mmWave Wireless Networks with 3D Beamforming

Mahdi Baianifar, S. Mohammad Razavizadeh, Hossein Akhlaghpasand, and Inkyu Lee

Abstract: **In this paper, we address the problem of 3D beamforming (3DBF) in millimeter wave (mmWave) wireless networks. In particular, we study the impact of base station (BS) antenna tilt angle optimization on the energy efficiency (EE) of mmWave networks under two different scenarios: a homogeneous network consisting of multiple macro base stations (MBSs), and a heterogeneous network where several femto base stations are added within the coverage areas of the MBSs. First, by adopting a stochastic geometry approach, we analyze the coverage probability of both scenarios that incorporate 3DBF. Then, we derive the EE of the networks as a function of the MBS antenna tilt angle. Next, optimization problems are formulated to maximize the EE of the networks by optimizing the tilt angle. Since the computational complexity of the optimal solution is very high, near-optimal low-complexity methods are proposed for solving the optimization problems. Simulation results show that in the mmWave networks, the 3DBF technique with optimized tilt angle can considerably improve the EE of the network. Also, the proposed low complexity approach presents a performance close to the optimal solution but with a significant reduced complexity.**

Index Terms: **3D beamforming, blockage effect, coverage probability, energy efficiency, heterogeneous network (HetNet), mmWave network, stochastic geometry, tilt angle optimization.**

I. INTRODUCTION

INCREASING demands for high data rate in the 5th generation (5G) cellular systems need much more bandwidth compared to current cellular networks. The millimeter wave (mmWave) frequency bands have recently attracted a lot of attentions due to large bandwidth that they offer [1], [2]. However, in practice they encounter some challenges including high path loss, high power consumptions and the blockage effect caused by buildings and human bodies [3]–[5]. Another emerging technique in 5G wireless networks is 3D beamforming (3DBF) which utilizes active large antenna arrays to control the antenna patterns in a 3D space [6]. In fact, in the 3DBF more degrees of freedom are exploited to adjust the beam patterns in both horizontal and vertical (tilt angle) domains to improve the network

performance in term of spectral efficiency and energy efficiency (EE) [6], [7]. On the other hand, due to the short wavelength of the mmWave bands, a large number of antenna elements can be packed in a small area arrays which makes them suitable for employing the 3DBF.

One of the recent powerful mathematical techniques that has been proposed for analyzing the performance of cellular networks is stochastic geometry (SG) [2], [9], [10]. This technique is widely used in evaluating different network performance metrics including coverage, capacity, spectral efficiency and the EE in the microwave as well as mmWave systems. An SG-based mathematical framework to model random blockage in the mmWave networks has been proposed in [3] in which the authors proved that the distribution of the number of the blockages in a link follows a Poisson distribution. In [2], the SG approach was employed for analyzing the coverage and rate of the mmWave networks and it was shown that the mmWave networks achieve a comparable coverage but higher data rates than microwave networks. Also, the SG technique was employed in [11] to evaluate the performance of multi-tier networks and it was shown that a sufficiently dense mmWave cellular network can outperform microwave cellular networks in terms of the coverage probability. In addition, the downlink of a multi-tier heterogeneous mmWave cellular network in a Nakagami fading channel was investigated by a SG approach in [12]. In [13], the effect of user association and power control on the coverage and EE of the mmWave system is investigated. The maximization of the EE by considering a constraint on the coverage probability is studied in [14] which provides insights for deployment of an energy efficient mmWave network.

In this paper, we address the problem of the 3DBF in the mmWave networks. In particular, our work focuses on the EE maximization in the mmWave networks by tilt angle optimization at the BSs that are equipped with active antenna systems. To the best of our knowledge, this problem has not been studied before in literature. Furthermore, for our analysis, we use a stochastic geometry approach. In this approach, the location of BSs are modelled by a homogeneous Poisson point process (PPP). In addition, we use a modified model for the propagation channel that properly incorporates the existence of blockage effect in the environment. Using the above assumptions and modeling, we first evaluate the signal-to-noise-plus-interference ratio (SINR) coverage probability and then derive the EE of the network as a function of the BSs' tilt angle.

We solve the above problem for two different scenarios. In the first scenario, a homogeneous network is studied where multiple macro base stations (MBSs) serve a number of macro-users. Applying the SG technique, we compute the coverage probability and the EE of the network. Afterwards, the optimum tilt

angle that maximizes the EE is found through an optimization problem. Because of the complex form of the objective function, this optimization problem is hard and can not be solved efficiently. The optimal value is then obtained by exhaustive search over the available range of tilt angles. In order to reduce the complexity, we propose an efficient algorithm based on bisection method which has a close performance to the exhaustive search but with a considerably reduced complexity.

The second scenario that we examine in this paper includes a two tier heterogeneous network (HetNet) composed of multiple MBSs and femto base stations (FBSs) which are modeled by two PPPs with different densities. To limit interference, we define a sleep region around each MBS so that the FBSs in the sleep regions do not transmit any signal. Using this idea, the coverage of the network is evaluated and the EE is calculated. Then, the MBS tilt angle and the radius of the sleep regions are jointly optimized through an optimization problem for maximizing the EE. We also propose an efficient method which considerably reduces the computational complexity. It is shown that the proposed efficient method has only a small degradation in the performance with respect to the optimal solution obtained by exhaustive search. In addition, in the second scenario, we provide a lower bound on the coverage probability of the femto users that is very tight.

Finally, through numerical simulations, we evaluate the performance of the proposed schemes and confirm that in a mmWave network, using the 3DBF technique with optimized tilt angle considerably improves the performance of the network in terms of the EE. Our simulations also demonstrate the effectiveness of the proposed low-complexity optimization methods.

The rest of the paper is organized as follows: In Section II, the system models of the homogeneous network and HetNet are described. Section III derives the coverage probabilities and EE of two scenarios. In Section IV, the EE maximization problem is formulated and the low-complexity solving method is presented. Numerical results are presented in Section V, and finally Section VI concludes the paper.

II. SYSTEM MODEL

We consider downlink of a multi-cell mmWave cellular network under two scenarios: A homogeneous network composed of multiple MBSs, and a two tier HetNet consisting of multiple MBSs and multiple FBSs that both the MBSs and FBSs utilize same frequencies in the mmWave bands. The path loss of the channels between the MBSs and macro users are given by [3]

$$L\left(r\right) = \begin{cases} C_L r^{-\alpha_L} & \text{with prob.} \quad P_L\left(r\right), \\ C_N r^{-\alpha_N} & \text{with prob.} \quad P_N\left(r\right), \end{cases} \qquad (1)$$

where C_L and C_N account for the path loss in a reference distance for line of sight (LOS) and non-LOS (NLOS) links, respectively, r is the distance between a BS and its associated user, and α_L and α_N denote the path loss exponents for LOS and NLOS links, respectively. Links are in the LOS condition with probability $P_L\left(r\right) = e^{-\beta r}$ where β indicates the intensity of the blockage effect; and in the NLOS condition with probability $P_N\left(r\right) = 1 - P_L\left(r\right)$ [3]. Also, it is assumed that the link between the MBSs and the femto users and that between
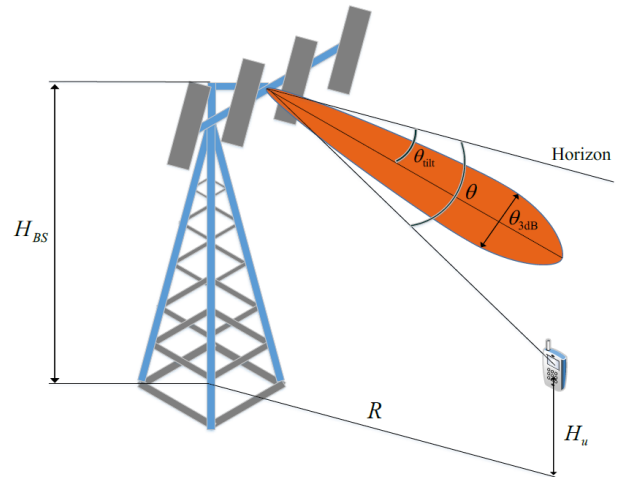

Fig. 1. Vertical antenna pattern at each BS.

FBSs and macro users are always in the NLOS condition. In addition, since femto users are usually located indoor, the channel between a femto user and interfering (non-serving) FBSs are assumed to be NLOS.

To design the 3DBF techniques, we need a model for the vertical and horizontal antenna patterns at the MBSs. In this paper, for the vertical plane, we adopt a model presented in [15] in which each MBS's antenna gain is expressed as

$$G\left(\theta, \theta_{\text{tilt}}\right) = -\min\left(12\left(\frac{\theta - \theta_{\text{tilt}}}{\theta_{\text{3dB}}}\right)^2, \text{SLL}_{\text{dB}}\right) \text{dB}, \qquad (2)$$

where $\theta \geq 0$ is the angle between the horizon and the line connecting the MBS to the user (see Fig. 1). In addition, $\theta_{\text{tilt}} \geq 0$, θ_{3dB}, and SLL_{dB} stand for the array tilt angle, the 3dB beamwidth, and the side-lobe level of the MBS antenna pattern in the vertical plane, respectively [16]. By defining $H_{\text{eff}} \triangleq H_{\text{BS}} - H_u$; where H_{BS} and H_u represent the MBSs' and users' antenna heights, respectively, (2) can be rewritten as

$$G\left(R, \theta_{\text{tilt}}\right) = -\min\left(12\left(\frac{\text{atan}\left(H_{\text{eff}}/R\right) - \theta_{\text{tilt}}}{\theta_{\text{3dB}}}\right)^2, \text{SLL}_{\text{dB}}\right) \text{dB},$$

where R equals the horizontal distance between the MBS and the user. It is assumed that all FBSs' and the users' antennas have an omni-directional pattern in the vertical domain.

For modeling the MBS's and macro users' antennas horizontal pattern, a sectorized pattern is utilized that has constant gains of M and m in its main-lobe and side-lobe, respectively [2]. The total antenna gain of a transmitter to receiver link in the horizontal plane is modelled by a random variable D which takes four values of $d_1 = M_t M_r$, $d_2 = M_t m_r$, $d_3 = m_t M_r$, and $d_4 = m_t m_r$ with probabilities $p_1 = c_t c_r$, $p_2 = c_t\left(1 - c_r\right)$, $p_3 = \left(1 - c_t\right) c_r$, and $p_4 = \left(1 - c_t\right)\left(1 - c_r\right)$, respectively. The subscripts t and r stand for the transmitter (MBS) and receiver (macro user), respectively. In addition, we have $c_t = \varphi_t/2\pi$ and $c_r = \varphi_r/2\pi$, in which φ_t and φ_r indicate the horizontal beamwidth of the transmitter and the receiver antennas, respectively. Also, we assume that antennas horizontal pattern for FBS and femto users are M^f and m^f in its main-lobe and side-lobe,

respectively with ϕ_t^f and ϕ_r^f as a horizontal beamwidth of the FBSs and femto users, respectively. We denote total antenna gain of the FBS and femto user by D^f which takes value d_i^f with probabilities p_i^f for $i = 1, \cdots, 4$, where they can be calculated in similar manner as the MBS and macro user. In the following, we explain these two scenarios for the mmWave network.

A. Homogeneous Cellular Network

In this scenario, only MBSs exist in the network whose positions are modeled by a homogeneous PPP Φ_m with density λ_m. From the Slivnyak theorem [17], to evaluate the performance of the network, it is sufficient to consider a typical user located at the origin and analyze its performance. The received signal at the typical user can be written as

$$y = \sqrt{P_m L_m (r_{0,0}) D_0 G_0} \cdot h_{0,0} \, s_0$$
$$+ \sum_{j \neq 0, \, X_j \in \Phi_m} \sqrt{P_m L_m (r_{j,0}) D_j G_j} \cdot h_{j,0} \, s_j + n, \quad (3)$$

where P_m represents the transmission power of each MBS and $r_{j,0}$, $L_m (r_{j,0})$ and $h_{j,0}$ indicate the distance, the path loss and the small scale fading between the jth MBS ($j = 0$ is for the MBS that serves the typical user) and the typical user, respectively, D_j is the total horizontal antenna gain between the jth MBS and the typical user, $G_j = G (r_{j,0}, \theta_{\text{tilt}})$ shows the vertical antenna gains, s_j equals the transmitted signal of the jth MBS, $n \sim \mathcal{CN} \left(0, \sigma^2\right)$ stands for the noise, and the location of the jth MBS is denoted by X_j. We consider Nakagami-m fading in which fading power $|h_{j,0}|^2$ follows a Gamma distribution $\Gamma (m, 1/m)$ with the following complementary cumulative distribution function (CCDF)

$$\bar{F} (z) = e^{-mz} \sum_{k=0}^{m-1} \frac{(mz)^k}{k!}.$$

In all equations, index 0 is used for identifying the typical user and also the MBS that serves this user.

B. Two Tier Heterogeneous Network

In this scenario, in addition to the MBSs, a number of FBSs exist in the network. The locations of the MBSs and FBSs are modeled by two independent homogeneous PPP Φ_m and Φ_f with densities λ_m and λ_f, respectively. Location of the jth FBS is denoted by Y_j. In this case, we analyze the performance of a typical macro user as well as a typical femto user. It is assumed that femto users are uniformly distributed within the coverage area of its serving FBS, which has a circular area of radius R_f. Defining the signal attenuation caused by walls as ℓ_W, the attenuation of the links between the MBSs and the typical indoor femto user and that between non-serving FBSs and the typical indoor femto user are represented as ℓ_W and $(\ell_W)^2$, respectively. To decrease interference on the macro users, we consider a sleep region with radius R_c around each MBS, where the FBSs lying in this region are forced to enter a sleep mode and do not transmit any signals. In other words, if the distance of a FBS from each MBS is less than R_c, it will be turned off. By considering the above assumptions, the received signal at the typical macro user and femto user respectively become

$$y_m = \sqrt{P_m L_m \left(r_{0,0}^m\right) D_0 G_0} \cdot h_{0,0} s_0$$
$$+ \sum_{j \neq 0, \, X_j \in \Phi_m} \sqrt{P_m L_m \left(r_{j,0}^m\right) D_j G_j} \cdot h_{j,0} s_j$$
$$+ \sum_{j, \, Y_j \in \Phi_f'} \sqrt{P_f \ell_W L_m^f \left(r_{j,0}^{fm}\right) D_j^{fm}} \cdot g_{j,0}^f x_j + n, \quad (4)$$

$$y_f = \sqrt{P_f L_f \left(r_{0,0}^f\right) D_0^f} \cdot g_{0,0} x_0$$
$$+ \sum_{j, \, X_j \in \Phi_m} \sqrt{P_m \ell_W L_f^m \left(r_{j,0}^{mf}\right) D_j^{mf} G_j} \cdot h_{j,0}^m s_j$$
$$+ \sum_{j \neq 0, \, Y_j \in \Phi_f'} \sqrt{P_f \left(\ell_W\right)^2 L_f \left(r_{j,0}^f\right) D_j^f} \cdot g_{j,0} x_j + n',$$

$$(5)$$

where $r_{j,0}^m$ and $r_{j,0}^{fm}$ denote the distance between the jth MBS and the typical macro user and that between the jth FBS and the typical macro user, respectively, $r_{j,0}^f$ and $r_{j,0}^{mf}$ show the distance between the jth FBS and the typical femto user and that between the jth MBS and the typical femto user, respectively, Φ_f' indicates the modified version of Φ_f after excluding the FBSs in radius of R_c of each MBS, $L_m^f (r_{j,0})$, D_j^{fm} and $g_{j,0}^f$ represent the path loss, the total antenna gain in the horizontal domain and the small scale fading between the typical macro user and the jth FBS, respectively, x_j stands for the transmitted signal of the jth FBS, $g_{j,0}$ and $L_f \left(r_{j,0}^f\right)$ equal the small scale fading and the path loss between the typical femto user and the jth FBS, respectively, D_j^f shows the total antenna gain between the jth FBS and the typical femto user, $L_f^m \left(r_{j,0}^{mf}\right)$, D_j^{mf} and $h_{j,0}^m$ represent the path loss, the total antenna gain in the horizontal domain and the small scale fading between the typical femto user and the jth MBS, respectively, P_f equals the transmitted power of the jth FBS, and n and n' are the complex Gaussian noise as $\mathcal{CN} \left(0, \sigma^2\right)$. We define the values of variable D^{fm} by $d_i^{fm}, i = 1, \cdots, 4$ with probabilities p_i^{fm} (calculations are similar to MBS and macro users total antenna gain). D^{mf} takes values d_i^{mf} with probabilities p_i^{mf}. Also, since these links are in NLOS condition, $g_{j,0}, g_{j,0}^f, h_{j,0}^m$ are distributed as $\mathcal{CN} (0, 1)$.

III. ENERGY EFFICIENCY CALCULATION

In this section, first the coverage probability of the network is calculated and then used for deriving the EE under two above scenarios. There exist different user association rules like the nearest BS, minimum path or the strongest average power and also maximum SINR [2], [18], [19] and in this paper, we use the maximum average received power user association rule in which each user is associated with the BS that provides it the strongest average received power. However, it should be noted that in the

mmWave networks, because of the blockage effect and different path loss exponents for LOS and NLOS conditions, the strongest BS is not necessarily the nearest BS. To address this issue, in our analyses, we first map each NLOS BS located at distance r from the origin to an equivalent LOS BS with a larger distance $R_{eq}(r) = (C_L/C_N)^{1/\alpha_L} r^{\alpha_N/\alpha_L}$, and then use the distance criterion to associate the users to the BSs. In addition, by considering different probabilities for LOS and NLOS links as in (1), the homogeneous PPP, Φ_m can be divided into two independent non-homogeneous PPPs, Φ_L and Φ_N with densities $\lambda_L(r) = \lambda_m P_L(r)$ and $\lambda_N(r) = \lambda_m P_N(r)$, respectively. The distance between the typical user and its serving BS is a random variable whose probability density function (PDF) is obtained by the following lemma.

Lemma 1: Assuming the highest power user association rule, the PDF of the distance between the typical user and its serving BS is given by (6) at the top of the next page, where $R_{eq}^{-1}(r) = \mu r^\kappa$, $\mu = (C_N/C_L)^{1/\alpha_N}$ and $\kappa = \alpha_L/\alpha_N$.

Proof: The CCDF of the distance of the nearest BS to the typical user R can be calculated as

$$
\begin{aligned}
&\Pr\{R > r\} \\
&= \Pr\{\Phi_m(B(0,r)) = 0\} \\
&= \Pr\{(\Phi_L(B(0,r)) = 0) \cap (\Phi_N(B(0, R_{eq}^{-1}(r))) = 0)\} \\
&= \Pr\{\Phi_L(B(0,r)) = 0\} \Pr\{\Phi_N(B(0, R_{eq}^{-1}(r))) = 0\},
\end{aligned}
\tag{7}
$$

where $B(0,r)$ shows a ball centering at origin with radius r, $\Phi_m(B(0,r))$ represents the number of PPP Φ_m in the ball $B(0,r)$, and the last equality comes from the fact that Φ_L and Φ_N are independent. Hence $\Pr\{\Phi_L(B(0,R)) = 0\}$ can be calculated as

$$
\begin{aligned}
&\Pr\{\Phi_L(B(0,r)) = 0\} \\
&\overset{(a)}{=} \exp\left(-\int_{B(0,r)} \lambda_L(\|x\|)\, dx\right) \\
&\overset{(b)}{=} \exp\left(-2\pi\lambda_m \int_0^r \rho P_L(\rho)\, d\rho\right) \\
&= \exp\left(-\frac{2\pi\lambda_m}{\beta^2}\left(1 - (1 + \beta r) e^{-\beta r}\right)\right),
\end{aligned}
\tag{8}
$$

where (a) is due to the null probability [20] and (b) comes from the definition of λ_L and $P_L(r)$. Following a similar approach, we can calculate $\Pr\{\Phi_N(B(0, R_{eq}^{-1}(r))) = 0\}$. Finally, by inserting into (7) and considering the fact that $f_R(r) = -\frac{d}{dr}\Pr\{R > r\}$, the proof is completed. $\square$

A. Homogeneous Cellular Network

From (3), the received SINR at the typical user is obtained as

$$
\text{SINR} = \frac{P_m L_m(r_{0,0}) D_0 G_0 |h_{0,0}|^2}{\sum_{j \neq 0,\, X_j \in \Phi_m} P_m L_m(r_{j,0}) D_j G_j |h_{j,0}|^2 + \sigma^2}.
$$

It is assumed that the main beam of the typical user and its serving MBS's antennas are aligned, and therefore $D_0 = M_t M_r$. Then, the coverage probability is calculated in the following the-

orem.

Theorem 1: The coverage probability of the typical user associated with the MBS that provides the highest received power is obtained as

$$
\begin{aligned}
&\mathcal{P}^c(\gamma, \theta_{\text{tilt}}) \\
&= \Pr\{\text{SINR} > \gamma\} \\
&= \int_0^\infty e^{-ms\sigma^2} \sum_{k=0}^{m-1} \sum_{\ell=0}^k C_{k,\ell}\left[\frac{d^\ell}{dz^\ell}\mathcal{L}_{I_{\Phi_m}}(z, \theta_{\text{tilt}})\right]_{z=ms} f_R(\rho)\, d\rho,
\end{aligned}
\tag{9}
$$

where s is defined as $s = \gamma\rho^{\alpha_L}/P_m C_L D_0 G_0$ and $C_{k,\ell} = (-1)^\ell \frac{(ms\sigma^2)^{k-\ell}}{k!}\binom{k}{\ell}$, γ is the SINR threshold for the typical user, and $\mathcal{L}_{I_{\Phi_m}}(z, \theta_{\text{tilt}})$ represents the Laplace transform of $I_{\Phi_m}(\theta_{\text{tilt}}) = \sum_{j \neq 0,\, X_j \in \Phi_m} P_m L_m(r_{i,0}) D_j G_j |h_{j,0}|^2$ as

$$
\begin{aligned}
&\mathcal{L}_{I_{\Phi_m}} \\
&= E_{I_{\Phi_m}}\left[\exp\left(-z I_{\Phi_m}(\theta_{\text{tilt}})\right)\right] \\
&= \prod_{i=1}^4 \exp\left(-C_i \int_\rho^\infty F_L(z, x, d_i, \theta_{\text{tilt}}) x P_L(x)\, dx\right) \\
&\quad \times \prod_{i=1}^4 \exp\left(-C_i \int_{R_{eq}^{-1}(\rho)}^\infty F_N(z, x, d_i, \theta_{\text{tilt}}) x P_N(x)\, dx\right).
\end{aligned}
\tag{10}
$$

Here we define $C_i = 2\pi\lambda_m p_i$ and

$$
\begin{aligned}
&F_w(z, x, d_i, \theta_{\text{tilt}}) \\
&= 1 - \frac{1}{\left(1 + \frac{z P_m C_w d_i G(x, \theta_{\text{tilt}})}{m x^{\alpha_w}}\right)^m}, \quad w \in \{L, N\}.
\end{aligned}
$$

Proof: $\mathcal{P}^c$ can be obtained as

$$
\begin{aligned}
&\mathcal{P}^c(\gamma, \theta_{\text{tilt}}) \\
&= E_{\rho, I_{\Phi_m}}\left\{\Pr\left\{\text{SINR} > \gamma \,\middle|\, r_{0,0} = \rho\right\}\right\} \\
&\overset{(a)}{=} E_{\rho, I_{\Phi_m}}\left\{\Pr\left\{|h_{0,0}|^2 > \frac{\gamma\rho^{\alpha_L}}{P_m C_L D_0 G_0}(I_{\Phi_m} + \sigma^2) \,\middle|\, r_{0,0} = \rho\right\}\right\} \\
&\overset{(b)}{=} E_{\rho, I_{\Phi_m}}\left\{e^{-ms(I_{\Phi_m} + \sigma^2)} \sum_{k=0}^{m-1} \frac{(ms(I_{\Phi_m} + \sigma^2))^k}{k!}\right\} \\
&= \int_0^\infty e^{-ms\sigma^2} \sum_{k=0}^{m-1} \sum_{\ell=0}^k C_{k,\ell}\left[\frac{d^\ell}{dz^\ell}\mathcal{L}_{I_{\Phi_m}}(z, \theta_{\text{tilt}})\right]_{z=ms} f_R(\rho)\, d\rho,
\end{aligned}
$$

where $E\{.\}$ denotes the expectation operator and (a) follows from $L_m(r_{0,0}) = C_L r_{0,0}^{-\alpha_L}$ for the maximum received power association method, and (b) comes from the fact that $|h_{0,0}|^2 \sim \Gamma(m, \frac{1}{m})$.

$$f_R(r) = 2\pi\lambda_m \left(r e^{-\beta r} + \mu\kappa r^{2\kappa-1} \left(1 - e^{-\beta R_{eq}^{-1}(r)} \right) \right) \times \exp\left(-\frac{2\pi\lambda_m}{\beta^2} \left(1 - (1+\beta r) e^{-\beta r} \right) \right)$$

$$\times \exp\left(-\frac{2\pi\lambda_m}{\beta^2} \left(\frac{\beta^2 \left(R_{eq}^{-1}(r) \right)^2}{2} + \left(\beta R_{eq}^{-1}(r) + 1 \right) e^{-\beta R_{eq}^{-1}(r)} - 1 \right) \right) \tag{6}$$

Also,

$$I_{\Phi_m} = \sum_{j\neq 0,\, X_j\in\Phi_L} P_m C_L r_{j,0}^{-\alpha_L} D_j G_j |h_{j,0}|^2$$
$$+ \sum_{j\neq 0,\, X_j\in\Phi_N} P_m C_N r_{j,0}^{-\alpha_N} D_j G_j |h_{j,0}|^2$$
$$= I_{\Phi_L} + I_{\Phi_N}.$$

Since Φ_L and Φ_N are independent, $\mathcal{L}_{I_{\Phi_m}}(s, \theta_{\text{tilt}})$ can be written as

$$\mathcal{L}_{I_{\Phi_m}}(s, \theta_{\text{tilt}}) = E_{I_{\Phi_m}} \{\exp(-sI_{\Phi_m})\}$$
$$= E_{I_{\Phi_L}} \{\exp(-sI_{\Phi_L})\} E_{I_{\Phi_N}} \{\exp(-sI_{\Phi_N})\}$$
$$= \mathcal{L}_{I_{\Phi_L}}(s) \mathcal{L}_{I_{\Phi_N}}(s). \tag{11}$$

Hence we calculate $\mathcal{L}_{I_{\Phi_L}}(s)$ as

$$\mathcal{L}_{I_{\Phi_L}}$$
$$= E_{I_{\Phi_L}} \left\{ \exp\left(-s \sum_{\substack{j\neq 0,\\ X_j\in\Phi_L}} P_m C_L r_{j,0}^{-\alpha_L} D_j G_j |h_{j,0}|^2 \right) \right\}$$
$$= E_{\Phi_L, h_{j,0}, D_j} \left\{ \prod_{\substack{j\neq 0,\\ X_j\in\Phi_L}} \exp\left(-s P_m C_L r_{j,0}^{-\alpha_L} D_j G_j |h_{j,0}|^2 \right) \right\}$$
$$\stackrel{(a)}{=} E_{\Phi_L} \left\{ \prod_{\substack{j\neq 0,\\ X_j\in\Phi_L}} E \left\{ \frac{1}{\left(1 + \frac{s}{m} P_m C_L r_{j,0}^{-\alpha_L} D_j G_j \right)^m} \right\} \right\}$$
$$\stackrel{(b)}{=} \prod_{i=1}^{4} \exp\left(-C_i \int_{\rho}^{\infty} F_L(s, v, d_i, \theta_{\text{tilt}}) v P_L(v)\, dv \right),$$

where (a) and (b) are derived from the fact $|h_{j,0}|^2 \sim \Gamma\left(m, \frac{1}{m}\right)$ and the definition of the total antenna gain in horizontal domain, and also from the probability generating functional (PGFL) of the PPP [17]. Then $\mathcal{L}_{I_{\Phi_N}}(s)$ is computed by a similar method. Substituting $\mathcal{L}_{I_{\Phi_L}}(s)$ and $\mathcal{L}_{I_{\Phi_N}}(s)$ into (11) with $s = \gamma\rho^{\alpha_L} / P_m C_L D_0 G_0$, the proof is completed. □

In the following, by using the coverage probability in (9), the EE of the network is calculated. The EE is defined as [21], [22]

$$\text{EE}(\theta_{\text{tilt}}) = \frac{\mathcal{P}^c(\gamma, \theta_{\text{tilt}}) \log_2(1+\gamma)}{P_{cm} + \eta_m P_m}, \tag{12}$$

where P_{cm} indicate the power consumption related to the signal processing and cooling, and η_m is the power amplifier efficiency

of each BS. By substituting (9) and (10) in (12), we have

$$\text{EE}(\theta_{\text{tilt}}) =$$
$$\frac{\int_0^\infty e^{-ms\sigma^2} E_{I_{\Phi_m}} \left[e^{-msI_{\Phi_m}} \sum_{k=0}^{m-1} \frac{\left(ms\left(I_{\Phi_m} + \sigma^2 \right) \right)^k}{k!} \right] f_R(\rho)\, d\rho}{P_{cm} + \eta_m P_m}. \tag{13}$$

B. Two Tier Heterogeneous Network

In this scenario, it is assumed that location of the MBSs and FBSs are modeled by two independent PPP, Φ_m and Φ_f with densities λ_m and λ_f, respectively. According to (4) and (5), the SINR in the typical macro and femto users are given as

$$\text{SINR}_m = \frac{P_m L_m \left(r_{0,0}^m \right) D_0 G_0 |h_{0,0}|^2}{I_{\Phi_m}^m + I_{\Phi_f'}^m + \sigma^2},$$

$$\text{SINR}_f = \frac{P_f L_f \left(r_{0,0}^f \right) D_0^f |g_{0,0}|^2}{I_{\Phi_m}^f + I_{\Phi_f'}^f + \sigma^2},$$

where

$$I_{\Phi_m}^m = \sum_{\substack{j\neq 0,\\ X_j\in\Phi_m}} P_m L_m \left(r_{j,0}^m \right) D_j G_j |h_{j,0}|^2,$$

$$I_{\Phi_f'}^m = \sum_{j,\, Y_j\in\Phi_f'} P_f \ell_W L_m^f \left(r_{j,0}^{fm} \right) D_j^{fm} |g_{j,0}^f|^2,$$

$$I_{\Phi_m}^f = \sum_{j,\, X_j\in\Phi_m} P_m \ell_W L_f^m \left(r_{j,0}^{mf} \right) D_j^{mf} G_j |h_{j,0}^m|^2,$$

$$I_{\Phi_f'}^f = \sum_{\substack{j\neq 0,\\ Y_j\in\Phi_f'}} P_f \left(\ell_W \right)^2 L_f \left(r_{j,0}^f \right) D_j^f |g_{j,0}|^2.$$

It is assumed that the main beam of the typical femto user and its serving FBS's antennas are aligned i.e., $D_0^f = M_t^f M_r^f$.

Because of sleep regions, the FBSs are modeled by a Poisson hole process. According to [20], Φ_f', has the density

$$\lambda_{f'} = \lambda_f \exp\left(-\lambda_m \pi R_c^2 \right).$$

The following theorem provides the coverage probability of the macro users.

Theorem 2: In the HetNet scenario, by considering the sleep region around each MBS, the coverage probability of a typical

macro user is expressed as

$$
\mathcal{P}_m^c \left(\gamma_m, \theta_{\text{tilt}}, R_c \right)
$$
$$
= \int_0^\infty \sum_{k=0}^{m-1} \sum_{\ell=0}^k C_{k,\ell} \left[\frac{d^\ell}{dz^\ell} \mathcal{L}_{I_{\Phi_{m,f}}} \left(z, \theta_{\text{tilt}} \right) \right]_{z=ms} f_R \left(\rho \right) d\rho,
$$
(14)

where $\mathcal{L}_{I_{\Phi_{m,f}}} \left(z, \theta_{\text{tilt}} \right) = \left(\mathcal{L}_{I_{\Phi_m}} \left(z, \theta_{\text{tilt}} \right) \mathcal{L}_{I_{\Phi_f'}^m} \left(z, \theta_{\text{tilt}} \right) \right)$ and $s = \gamma_m \rho^{\alpha_L} / P_m C_L D_0 G_0$, γ_m represents the SINR threshold for the typical macro user and $\mathcal{L}_{I_{\phi_f'}^m} \left(z, \theta_{\text{tilt}} \right)$ indicates the Laplace transform of the interference from the FBSs to the macro user as

$$
\mathcal{L}_{I_{\phi_f'}^m} = \prod_{i=1}^4 \exp \left(-C_i^{f'} \left(s P_f \ell_W C_N d_i^{fm} \right)^{\frac{2}{\alpha_N}} \frac{\pi}{\alpha_N \sin \left(\frac{2\pi}{\alpha_N} \right)} \right),
$$
(15)

where $C_i^{f'} = 2\pi \lambda_{f'} p_i^{fm}$.

Proof: Adopting a similar approach to Theorem 1, we have

$$
\mathcal{P}_m^c \left(\gamma_m, \theta_{\text{tilt}}, R_c \right)
$$
$$
= \Pr \left\{ \text{SINR}_m > \gamma_m \right\}
$$
$$
= \int_0^\infty \Pr \left\{ \frac{P_m C_L r^{-\alpha_L} D_0 G_0 |h_{0,0}|^2}{I_{\Phi_m}^m + I_{\Phi_f'}^m + \sigma^2} > \gamma_m \middle| r = \rho \right\} f_R \left(\rho \right) d\rho.
$$

We can compute the probability inside the integral as

$$
\Pr \left\{ \frac{P_m C_L r^{-\alpha_L} D_0 G_0 |h_{0,0}|^2}{I_{\Phi_m} + I_{\Phi_f'}^m + \sigma^2} > \gamma_m \mid r = \rho \right\}
$$
$$
= \sum_{k=0}^{m-1} \sum_{\ell=0}^k C_{k,\ell} \left[\frac{d^\ell}{dz^\ell} \left(\mathcal{L}_{I_{\Phi_m}} \left(z, \theta_{\text{tilt}} \right) \mathcal{L}_{I_{\Phi_f'}^m} \left(z, \theta_{\text{tilt}} \right) \right) \right]_{z=ms},
$$

where we use the fact that $|h_{0,0}|^2$ has Gamma distribution. Similarly, we have

$$
\mathcal{L}_{I_{\Phi_f'}^m}
$$
$$
= E \left\{ \exp \left(-s \sum_{j, Y_j \in \Phi_f'} P_f \ell_W C_N \left(r_{j,0}^{fm} \right)^{-\alpha_N} D_j^{fm} |g_{j,0}^f|^2 \right) \right\}
$$
$$
\overset{(a)}{=} E_{\Phi_f', D_j^{fm}} \left\{ \prod_{j, Y_j \in \Phi_f'} \frac{1}{1 + s P_f \ell_W C_N \left(r_{j,0}^{fm} \right)^{-\alpha_N} D_j^{fm}} \right\}
$$
$$
\overset{(b)}{=} \prod_{i=1}^4 \exp \left(-C_i^{f'} \int_0^\infty \frac{x}{1 + \left(s P_f \ell_W C_N d_i^{fm} \right)^{-1} x^{\alpha_N}} dx \right),
$$

where (a) is due to the fact $|g_{j,0}^f|^2 \sim \exp(1)$ and (b) is derived from the PGFL of the PPP Φ_f' [17]. □

Next, we derive the coverage probability of the typical femto

user in the following theorem.

Theorem 3: In the HetNet scenario, the coverage probability of the typical femto user is expressed as

$$
\mathcal{P}_f^c \left(\gamma_f, \theta_{\text{tilt}}, R_c \right) = \exp \left(-\pi \lambda_m R_c^2 \right)
$$
$$
\times \int_0^{R_f} e^{-s_f \sigma^2} \mathcal{L}_{I_{\Phi_m}^f} \left(s_f, \theta_{\text{tilt}} \right) \mathcal{L}_{I_{\phi_f'}^f} \left(s_f, \theta_{\text{tilt}} \right) g_R \left(\rho \right) d\rho d\rho,
$$
(16)

where $s_f = \left(\gamma_f / (P_f C_L D_0^f) \right) \cdot \rho^{\alpha_L}$, γ_f denotes the SINR threshold for the typical femto user, and $\mathcal{L}_{I_{\Phi_m}^f} \left(s_f, \theta_{\text{tilt}} \right)$ and $\mathcal{L}_{I_{\Phi_f'}^f} \left(s_f, \theta_{\text{tilt}} \right)$ are obtained as

$$
\mathcal{L}_{I_{\Phi_m}^f} = \prod_{i=1}^4 \exp \left(-C_i^{mf} \int_0^\infty \frac{x}{1 + \frac{x^{\alpha_N}}{s_f P_m \ell_W C_N d_i^{mf} G(x, \theta_{\text{tilt}})}} dx \right),
$$
(17)

$$
\mathcal{L}_{I_{\Phi_f'}^f} = \prod_{i=1}^4 \exp \left(-2\pi \lambda_{f'} p_i^f \int_\rho^\infty \frac{x}{1 + \frac{x^{\alpha_N}}{s_f P_f (\ell_W)^2 C_N d_i^f}} dx \right),
$$
(18)

where $C_i^{mf} = 2\pi \lambda_m p_i^{mf}$ and $g_R \left(\rho \right) = 2\rho / R_f^2$.

Proof: According to the hole point process, the probability that a FBS outside of a sleep region is active equals $\exp \left(-\pi \lambda_m R_c^2 \right)$. Thus we have

$$
\mathcal{P}_f^c \left(\gamma_f, \theta_{\text{tilt}}, R_c \right) = \exp \left(-\pi \lambda_m R_c^2 \right) \Pr \left\{ \text{SINR}_f > \beta_f \right\}. \quad (19)
$$

The rest of calculation is similar to Theorem 2 and thus is not repeated here. □

In the following lemma, we derive a lower bound on the terms of the coverage probability of the typical femto user.

Lemma 2: In the HetNet scenario, $\mathcal{L}_{I_{\Phi_m}^f}$ and $\mathcal{L}_{I_{\Phi_m'}^f}$ in (17) and (18) can be respectively lower bounded as

$$
\mathcal{L}_{I_{\Phi_m}^f}
$$
$$
\geq \exp \left(-2\pi \lambda_m \left(s_f P_m \ell_w C_N G_{\max} \right)^{\frac{2}{\alpha_N}} \frac{\pi E \left\{ D^{mf \frac{2}{\alpha_N}} \right\}}{\alpha_N \sin \frac{2\pi}{\alpha_N}} \right),
$$
(20)

$$
\mathcal{L}_{I_{\Phi_m'}^f}
$$
$$
\geq \exp \left(-2\pi \lambda_{f'} \left(s_f P_f (\ell_w)^2 C_N \right)^{\frac{2}{\alpha_N}} \frac{\pi E \left\{ D^{f \frac{2}{\alpha_N}} \right\}}{\alpha_N \sin \frac{2\pi}{\alpha_N}} \right).
$$
(21)

Proof: To find a lower bound for (17), we replace $G(x, \theta)$ by its maximum value $G_{\max}$ which results in (20). Furthermore, to obtain a lower bound for (18), we use the fact that for any $f(x) \geq 0$ and $\rho \geq 0$, $\int_\rho^\infty f(x) dx \leq \int_0^\infty f(x) dx$ which results in (21). Also, we have $E \left\{ D^{\frac{2}{\alpha_N}} \right\} = \sum_{i=1}^4 p_i d_i^{\frac{2}{\alpha_N}}$. □

Corollary 1: A lower bound on the coverage probability of the typical femto user in (16) in an interference limited regime

(i.e. $\sigma^2 \approx 0$) is given by

$$\mathcal{P}_f^c (\gamma_f, \theta_{\text{tilt}}, R_c) \geq C_0 e^{-\pi \lambda_m R_c^2}, \qquad (22)$$

where C_0 is obtained as

$$C_0 = \left(\frac{\alpha_N}{\alpha_L} R_f^2 (C_1 + C_2)^{\frac{\alpha_N}{\alpha_L}} \right) \cdot \gamma \left(\frac{\alpha_N}{\alpha_L}, (C_1 + C_2) R_f^{\frac{2\alpha_L}{\alpha_N}} \right),$$

$\gamma(.,.)$ denotes the lower incomplete gamma function, and C_1 and C_2 are defined as

$$C_1 = 2\pi \lambda_m \left(\frac{\gamma_f P_m \ell_w C_N}{P_f C_L D_0^f} \right)^{\frac{2}{\alpha_N}} \frac{\pi}{\alpha_N \sin \frac{2\pi}{\alpha_N}} E \left\{ D^{mf \frac{2}{\alpha_N}} \right\},$$

$$C_2 = 2\pi \lambda_{f'} \left(\frac{\gamma_f (\ell_w)^2 C_N}{C_L D_0^f} \right)^{\frac{2}{\alpha_N}} \frac{\pi}{\alpha_N \sin \frac{2\pi}{\alpha_N}} E \left\{ D^{f \frac{2}{\alpha_N}} \right\},$$

respectively.

Proof: By substituting (20) and (21) into (16) and considering an interference limited regime ($\sigma^2 \approx 0$), the proof is complete. $\square$

In this scenario, the EE of the network is written as

$$\text{EE}(\theta_{\text{tilt}}) = \frac{\sum_{i \in \{m,f\}} \lambda_i \mathcal{P}_i^c (\gamma_i, \theta_{\text{tilt}}, R_c) \log_2 (1 + \gamma_i)}{\sum_{i \in \{m,f\}} \lambda_i (P_{ci} + \eta_i P_i)}, \quad (23)$$

where P_f and P_{cf} respectively represent the transmitted power and the constant power consumption in the FBSs and η_f is a constant related to the power amplifiers efficiency of the FBSs.

IV. ENERGY EFFICIENCY MAXIMIZATION

As we see in (12) and (23), the EE is a function of θ_{tilt} and therefore, it can be maximized by optimizing the tilt angle. The optimum tilt angle of the BSs is obtained through the following optimization problem

$$\underset{\theta_{\text{tilt}}}{\text{maximize}} \quad EE(\theta_{tilt}) \qquad (24)$$
$$\text{s.t.} \qquad 0 \leq \theta_{\text{tilt}} \leq 90°.$$

Unfortunately, the objective function of this problem is very complex and in the following, we propose low complexity algorithms for finding the optimal tilt angle in both scenarios.

A. Homogeneous Cellular network

In fact, to calculate the EE in this scenario, we first need to obtain $E_{I_{\Phi_m}} \left[e^{-ms I_{\Phi_m}} \sum_{k=0}^{m-1} \frac{(ms(I_{\Phi_m} + \sigma^2))^k}{k!} \right]$ by (10) for each value of ρ. Then, the integral at the numerator (13) must be calculated. Hence, the optimum tilt angle can not be found by an efficient method and we have to perform an exhaustive search over all possible values of θ_{tilt} which in this case is very hard to implement.

To address this problem, in the following, we propose a low-complexity method for finding the optimum tilt angle. As it is seen in (9), for calculating the coverage probability, we need to
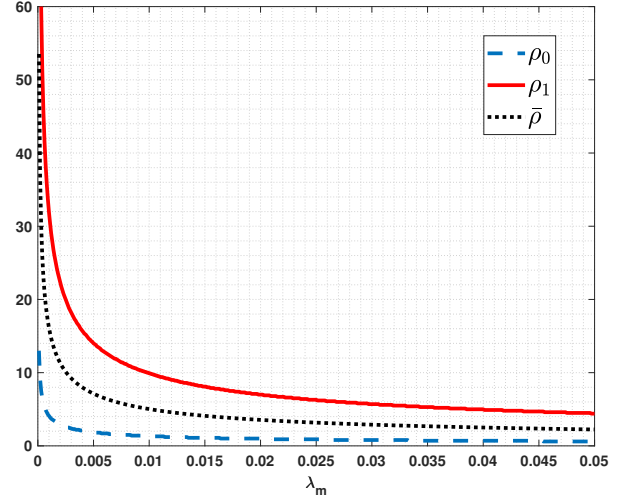

Fig. 2. The values of ρ_0, ρ_1 and $\bar{\rho}$ versus λ_m (for $\beta = 3 \times 10^{-3}$).

compute $E_\rho \left\{ e^{-ms\sigma^2} \sum_{k=0}^{m-1} \sum_{\ell=0}^{k} C_{k,\ell} \left[\frac{d^\ell}{dz^\ell} \mathcal{L}_I (z, \theta_{\text{tilt}}) \right]_{z=ms} \right\}$. By considering the PDF of R (i.e., the distance between the typical user and its serving BS) in (6), we define two distance bounds of ρ_0 and ρ_1 such that $\Pr\{\rho_0 \leq R \leq \rho_1\} \geq 1 - \epsilon$. Using these bounds, the optimal tilt angle will be restricted to the following range

$$\max \left\{ \text{atan} \left(\frac{H_{\text{eff}}}{\rho_1} \right) - \theta_0, 0 \right\} \leq \theta_{\text{tilt}} \leq \text{atan} \left(\frac{H_{\text{eff}}}{\rho_0} \right) + \theta_0, \qquad (25)$$

where $\theta_0 = \theta_{\text{3dB}} \sqrt{\text{SLL}_{\text{dB}}/12}$. The values of ρ_0 and ρ_1 can be obtained numerically using (6) for a given ϵ. In Fig. 2, we depict the values of these two bounds for $\epsilon = 0.1$ in different densities of the BSs, λ_m. In addition, the average distance between the typical user and its serving BS, i.e., $\bar{\rho} = E\{\rho\}$ is also shown in this figure. It is interesting to note that in large values of λ_m (which is related to dense mmWave networks), both of ρ_0 and ρ_1 converge to $\bar{\rho}$. We exploit this property to simplify the calculations.

Using the above property, we can apply the Taylor expansion at the point of $\bar{\rho}$ to obtain the following approximation for (9) as

$$E_\rho \left\{ e^{-ms\sigma^2} \sum_{k=0}^{m-1} \sum_{\ell=0}^{k} C_{k,\ell} \left[\frac{d^\ell}{dz^\ell} \mathcal{L}_I (z, \theta_{\text{tilt}}) \right]_{z=ms} \right\}$$
$$= E_\rho \left\{ \sum_{n=0}^{\infty} \frac{(\rho - \bar{\rho})^n}{n!} \right.$$
$$\left. \times \frac{d^n}{d\rho^n} \left(e^{-ms\sigma^2} \sum_{k=0}^{m-1} \sum_{\ell=0}^{k} C_{k,\ell} \left[\frac{d^\ell}{dz^\ell} \mathcal{L}_I (z,, \theta_{\text{tilt}}) \right]_{z=ms} \right) \bigg|_{\bar{\rho}} \right\}$$
$$\approx e^{-m\bar{s}\sigma^2} \sum_{k=0}^{m-1} \sum_{\ell=0}^{k} \frac{(m\bar{s}\sigma^2)^{k-\ell}}{k!} \binom{k}{\ell} (-1)^\ell \left[\frac{d^\ell}{dz^\ell} \mathcal{L}_I' (z, \theta_{\text{tilt}}) \right]_{z=m\bar{s}}, \qquad (26)$$

Algorithm 1: Bisection method.

1: Initialize $\theta_{\text{tilt}}^{\min} = \theta_{\min}$ and $\theta_{\text{tilt}}^{\max} = \theta_{\max}$.

2: Calculate $\mathcal{L}'_{I_{\Phi_m}}$ for $\theta_{\text{tilt}} = \frac{\theta_{\text{tilt}}^{\min} + \theta_{\text{tilt}}^{\max}}{2}$.

3: If resulted $\mathcal{L}_{I_{\Phi_m}}$ is greater than the result for $\theta_{\text{tilt}}^{\min}$, then set $\theta_{\text{tilt}}^{\min} = \theta_{\text{tilt}}$. Otherwise set $\theta_{\text{tilt}}^{\max} = \theta_{\text{tilt}}$

4: Stop when $\left|\theta_{\text{tilt}}^{\min} - \theta_{\text{tilt}}^{\max}\right|$ is less than a predefined value.

---

where $\bar{s} = \gamma \bar{\rho}^{\alpha_L} / C_L P_o D_0 G_0$ and

$$
\mathcal{L}'_{I_{\Phi_m}}(z, \theta_{\text{tilt}})
$$

$$
= \prod_{i=1}^{4} \exp\left(-2\pi \lambda_m p_i \int_{\bar{\rho}}^{\infty} F_L(z, x, d_i, \theta_{\text{tilt}})\, x P_L(x)\, dx \right)
$$

$$
\times \prod_{i=1}^{4} \exp\left(-2\pi \lambda_m p_i \int_{R_{eq}^{-1}(\bar{\rho})}^{\infty} F_N(z, x, d_i, \theta_{\text{tilt}})\, x P_N(x)\, dx \right).
$$
(27)

In addition to the above approximation, another way to reduce the complexity of the optimization problem in (24), is narrowing the search interval of θ_{tilt}. From (25) and considering that in the dense mmWave networks, both ρ_0 and ρ_1 converge to $\bar{\rho}$, we can obtain the bounds of θ_{tilt} as $\theta_{\min} \le \theta_{\text{tilt}} \le \theta_{\max}$, where

$$
\theta_{\min} = \max\left(0, \operatorname{atan}\left(\frac{H_{\text{eff}}}{\bar{\rho}} \right) - \theta_0 \right),
$$

$$
\theta_{\max} = \operatorname{atan}\left(\frac{H_{\text{eff}}}{\bar{\rho}} \right) + \theta_0.
$$
(28)

Therefore, an equivalent problem for (24) can be expressed as

$$
\underset{\theta_{\text{tilt}}}{\text{maximize}}
$$

$$
\frac{e^{-m\bar{s}\sigma^2} \sum_{k=0}^{m-1} \sum_{\ell=0}^{k} \frac{(m\bar{s}\sigma^2)^{k-\ell}}{k!} \binom{k}{\ell}(-1)^{\ell}\left[\frac{d^{\ell}}{dz^{\ell}} \mathcal{L}'_I(z, \theta_{\text{tilt}}) \right]_{z=m\bar{s}}}{P_c + \eta_m P_0}
$$

$$
\text{s.t.} \qquad \theta_{\min} \le \theta_{\text{tilt}} \le \theta_{\max}.
$$
(29)

This problem has a significantly reduced computational complexity compared to the original problem in (24). Since, we do not need to compute (10) for each value of ρ. In addition, the search interval is also limited. It can be shown that (29) is a convex problem and hence, it can be solved efficiently. In Algorithm 1, we present a bisection method to solve it. In Section V, we will show that the performance of the proposed low-complexity approach is very close to the optimal solution found by exhaustive search.

B. Two Tier Heterogeneous Network

As mentioned in Section III, in the HetNet scenario, to improve the coverage of the macro users, a sleep region with radius R_c is introduced around each MBS. On the other hand, when we turn off some FBSs, the coverage of the typical femto user decreases. As a result, we have a tradeoff between the coverage probabilities of the macro and femto users. Therefore, in our optimization problem, the radius of the sleep region should be

considered as an optimization parameter in addition to the tilt angle, and the EE maximization problem becomes

$$
\max_{\theta_{\text{tilt}}, R_c} \quad \frac{\sum_{i \in \{m,f\}} \lambda_i \mathcal{P}_i^c(\gamma_i, \theta_{\text{tilt}}, R_c) \log_2(1 + \gamma_i)}{\sum_{i \in \{m,f\}} \lambda_i (P_{ci} + \eta_i P_i)}
$$

$$
\text{s.t.} \quad \mathcal{P}_m^c \ge 1 - \epsilon_m, \quad \mathcal{P}_f^c \ge 1 - \epsilon_f,
$$

$$
0 \le \theta_{\text{tilt}} \le 90°, \quad 0 \le R_c \le R_c^{\max},
$$
(30)

where ϵ_m and ϵ_f are the minimum coverage requirements in the typical macro and femto users, respectively, and $R_c^{\max}$ denotes the maximum radius of the sleep region which is equal to $R_c^{\max} = 1/\sqrt{\pi \lambda_m}$. Again, this optimization problem is too complex to solve numerically.

To reduce the complexity of the above optimization problem, we follow a similar approach as in the homogeneous scenario. To this end, we consider the following optimization problem

$$
\max_{\theta_{\text{tilt}}, R_c} \quad \frac{\lambda_m \mathcal{P}_m^{c'} \log_2(1 + \gamma_m) + \lambda_{f'} \mathcal{L}'_{I_{\Phi_m}^f} \mathcal{L}'_{I_{\Phi_f'}^f} \log_2(1 + \gamma_f)}{\lambda_m (P_{cm} + \eta_m P_m) + \lambda_f (P_{cf} + \eta_f P_f)}
$$

$$
\text{s.t.} \quad \mathcal{L}'_{I_{\Phi_m}} \mathcal{L}'_{I_{\Phi_f'}^m} \ge 1 - \epsilon_m, \quad e^{-\pi \lambda_m R_c^2} \mathcal{L}'_{I_{\Phi_m}^f} \mathcal{L}'_{I_{\Phi_f'}^f} \ge 1 - \epsilon_f
$$

$$
0 \le \theta_{\text{tilt}} \le 90°, 0 \le R_c \le R_c^{\max},
$$
(31)

where

$$
\mathcal{P}_m^{c'} = \sum_{k=0}^{m-1} \sum_{\ell=0}^{k} \frac{(m\bar{s}\sigma^2)^{k-\ell}}{k!} \binom{k}{\ell}(-1)^{\ell}
$$

$$
\times \left[\frac{d^{\ell}}{dz^{\ell}} \left(\mathcal{L}'_{I_{\Phi_m}}(z, \theta_{\text{tilt}}) \mathcal{L}'_{I_{\Phi_f'}^m}(z, \theta_{\text{tilt}}) \right) \right]_{z=m\bar{s}}.
$$

Here we define

$$
\mathcal{L}'_{I_{\Phi_f'}^m}
$$

$$
= \prod_{i=1}^{4} \exp\left(-2\pi \lambda_{f'} p_i^{fm}\left(\bar{s} P_f \ell_w C_N d_i^{fm} \right)^{\frac{2}{\alpha_N}} \frac{\pi}{\alpha_N \sin \frac{2\pi}{\alpha_N}} \right),
$$
(32)

$$
\mathcal{L}'_{I_{\Phi_m}^f}
$$

$$
= \prod_{i=1}^{4} \exp\left(-2\pi \lambda_m p_i^{mf} \int_0^{\infty} \frac{x\, dx}{1 + \frac{x^{\alpha_N}}{\bar{s}_f P_m \ell_w C_N d_i^{mf} G(x, \theta_{\text{tilt}})}} \right),
$$
(33)

$$
\mathcal{L}'_{I_{\Phi_f'}^f}
$$

$$
= \prod_{i=1}^{4} \exp\left(-2\pi \lambda_{f'} p_i^{f} \int_{\bar{g}}^{\infty} \frac{x\, dx}{1 + \frac{x^{\alpha_N}}{\bar{s}_f P_f (\ell_w)^2 C_N d_i^{f}}} \right),
$$
(34)

where $\bar{g} = E\{g_R(\rho)\}$ and $\bar{s}_f = \frac{\gamma_f}{P_f C_L D_0} \bar{g}^{\alpha_L}$. By using this approach, the calculations are significantly simplified compared to the optimum exhaustive search. Here, instead of calculating (14) and (16) in which we need to compute (10), (15), (17) and (18) for all values of ρ, it is sufficient to evaluate (27) and (32) only for $\rho = \bar{\rho}$ and obtain (33) and (34) only for $\rho = \bar{g}$. In the
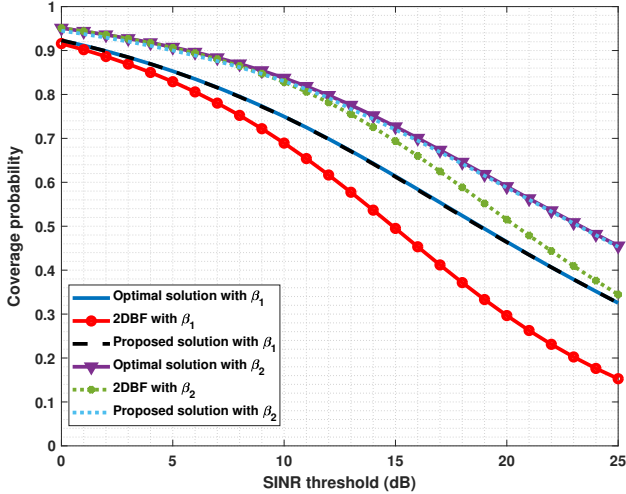
Table 1. Simulation parameters.

Parameter	Value	Parameter	Value
SLL_{dB}	20 dB	θ_{3dB}	$6°$
α_N	4	α_L	2.5
P_f, P_{fc}	100 mW, 9.6 W	η_f	4
P_m, P_{mc}	20, 68.73 W	η_m	3.77
(M_r, m_r, θ_r)	$(10\text{ dB}, -10\text{ dB}, 90°)$	(M_t, m_t, θ_t)	$(10\text{ dB}, -10\text{ dB}, 30°)$
$\left(M_r^f, m_r^f, \theta_r^f\right)$	$(10\text{ dB}, -10\text{ dB}, 90°)$	$\left(M_t^f, m_t^f, \theta_t^f\right)$	$(10\text{ dB}, -10\text{ dB}, 30°)$
β_1, β_2	$0.003, 0.006$	R_f	30 m

Fig. 3. Comparison of the coverage probability of the proposed low-complexity approach and the optimal solution and with the 2DBF.
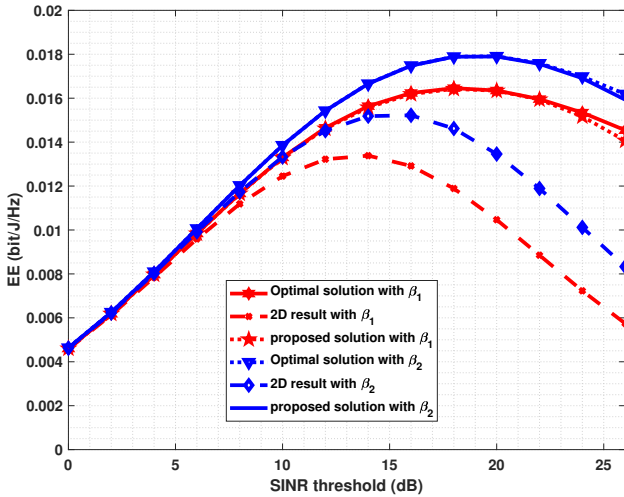
Fig. 4. EE comparison of the proposed low-complexity approach and the optimal solution and with the 2DBF.

next section, we will show that by applying this low-complexity approach, only a minor degradation in the performance is observed.

V. NUMERICAL RESULT

In this section, we numerically evaluate the performance of the proposed 3DBF with tilt angle optimization scheme for the mmWave networks. Through the simulations, we demonstrate that how the EE of the network is improved when the tilt angle of the BSs' antenna is optimized. In addition, the performance of the proposed low-complexity method is compared with the optimal solution obtained by exhaustive search. Table 1 summarizes the simulation parameters used in this section [3], [22].

We first examine the homogeneous scenario. The coverage probability of the network under this scenario is depicted in
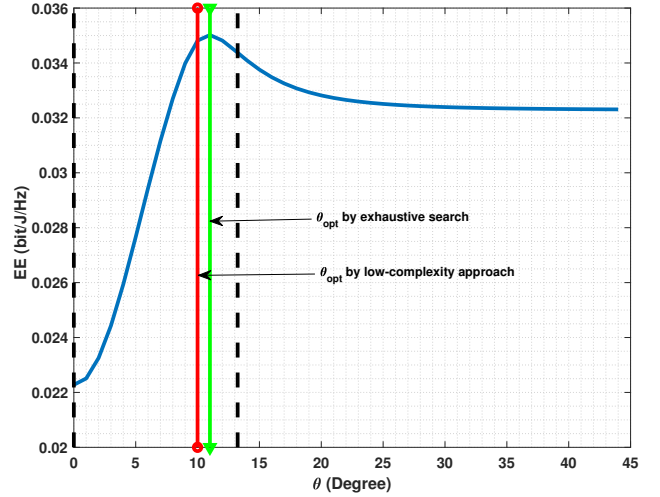

Fig. 5. EE comparison with respect to the BS tilt angle $\beta = \beta_1$, $\gamma = 20$ dB, $\lambda_m = 5.093 \times 10^{-6}$.

Fig. 3 as a function of the SINR threshold. The density of the MBS is $\lambda_m = 4.973 \times 10^{-5}$ and the curves are obtained under two different values of the blockage effect intensity β as in table 1 and $m = 5$. It is observed that by increasing the 3DBF outperforms in comparison with the network in which the tilt angle is not optimized (marked as 2DBF in the figure) and also the proposed low complexity method have performance close the optimal solution resulted from the exhaustive search.

Fig. 4 illustrates the EE of the network in terms of the SINR threshold for $\lambda_m = 8 \times 10^{-4}$ and two values of β as in Table 1 under this scenario with $m = 1$. As we see in this figure, the EE of the network that adopts 3DBF is always improved in comparison with the 2DBF. This improvement is more than 100% in high SINR thresholds. In addition, in this figure, the EE performance of the proposed low-complexity method is compared with the optimum method based on the exhaustive search. As we see in the figure, the performance of the proposed low-complexity approach is the same as the optimal solution in almost all the SINR threshold and for both values of β.

Fig. 5 presents the network EE with respect to the tilt angle for $\lambda_m = 5.093 \times 10^{-6}$ and $m = 5$. In this figure, the optimum tilt angles obtained by exhaustive search and the proposed low-complexity method are shown. Also, the dashed lines represent the tilt angle bounds obtained in (28). We see that both tilt angles are almost the same.

In Fig. 6, performance of the HetNet scenario is evaluated. This figure exhibits the effect of the FBSs density λ_f and the radius of the sleep region R_c on the optimum tilt angle that max-
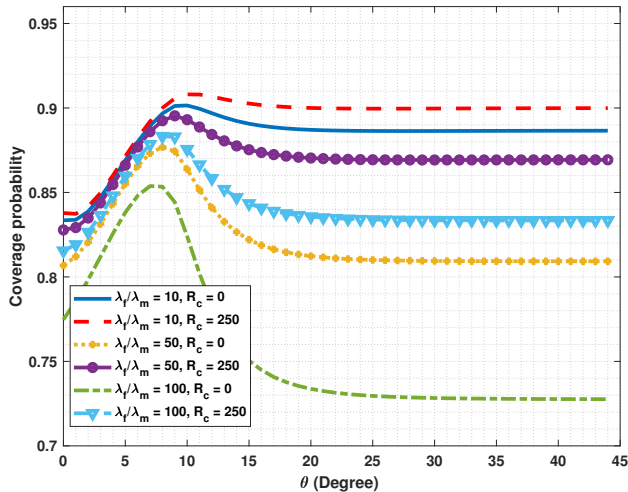
Fig. 6. The coverage probability of the typical macro user with various λ_f and R_c ($\lambda_m = 5.093 \times 10^{-6}, \beta = \beta_1$).

Fig. 8. Comparison of the optimal EE for different values of the blockage parameter ($\lambda_m = 4.973 \times 10^{-5}$).
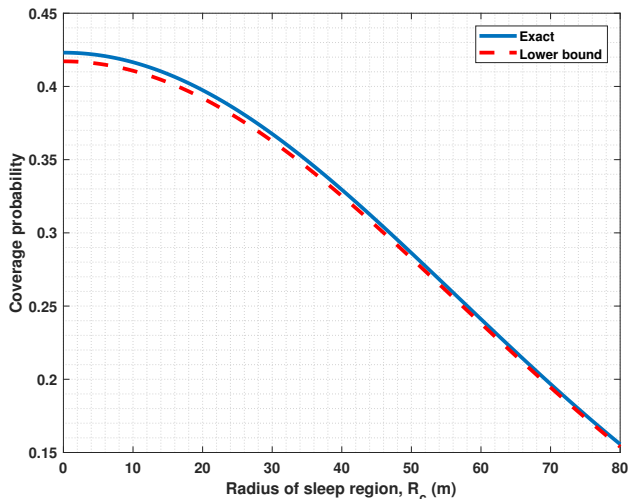

Fig. 7. Comparison of the exact coverage probability of the typical femto user and its lower bound with $\lambda_f = 10\lambda_m$ ($\lambda_m = 4.973 \times 10^{-5}$), $\sigma^2 = 5 \times 10^{-4}$ (SNR$_f = 23$ dB).

Fig. 9. Comparison of the optimal R_c for different values of the blockage parameter ($\lambda_m = 4.973 \times 10^{-5}$).

imizes the coverage of the typical macro user. In this figure we see that by increasing the density of the FBSs, the optimum tilt angle slightly decreases. Also by increasing R_c or reducing the density of the FBSs, the coverage probability of the macro users increases, since interference from the FBSs is reduced.

Fig. 7 illustrates the coverage probability of the typical femto user in terms of R_c for case of $\sigma^2 = 5 \times 10^{-4}$, which corresponds to SNR$_f = P_f/\sigma^2 = 23$ dB. In this figure, we see that the lower bound obtained in (30) is very tight. It is observed that although the lower bound is obtained under assumption of an interference limited scenario, it is still quite tight in other scenarios.

Figs. 8 and 9 plot the optimal EE, the optimal radius of the sleep region and the optimal tilt angle, respectively, with
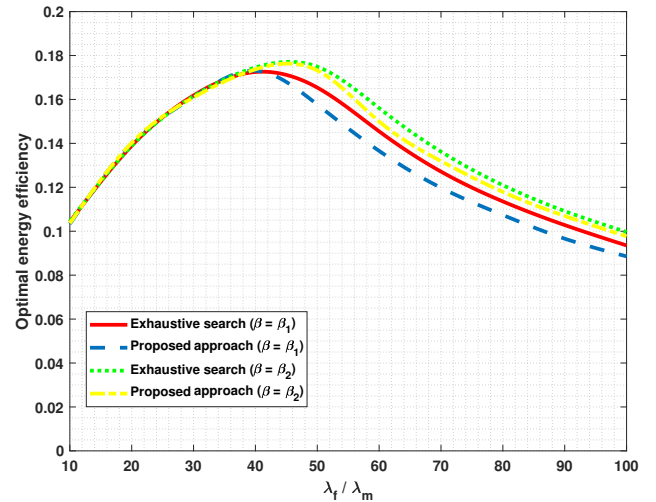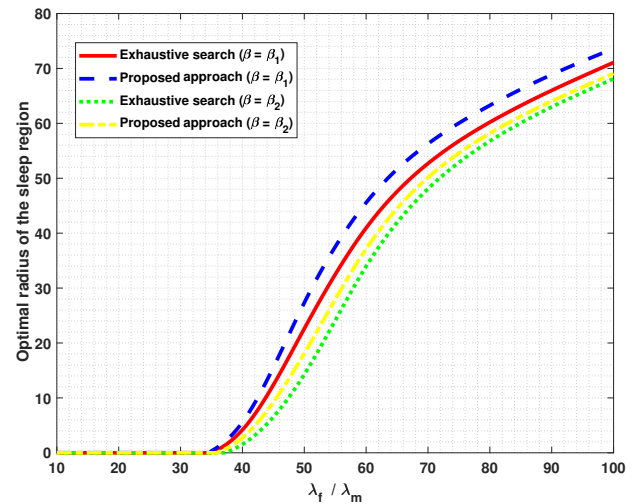
$\epsilon_m = 0.2, \epsilon = 0.7, \gamma_m = \gamma_f = 10$ dB. We can check that the proposed low complexity approach has only a minor degradation in the performance with respect to the exhaustive search.

VI. CONCLUSION

In this paper, we have studied the EE maximization problem in the downlink of a 3D beamforming mmWave network. We have optimized the tilt angle of the BSs to maximize the EE in a homogeneous network and a two tier HetNet mmWave cellular network. In both scenarios, we have optimized the tilt angle of the MBS's antenna to maximize the EE. In addition, in the second scenario, the optimization of the radius of the sleep region has also been considered. In addition, to reduce the complexity of the optimization problems, an efficient method based on bi-section algorithm has been proposed to compute the optimal tilt

angle. The proposed algorithms result in almost the same EE performance as the optimal method based on exhaustive search but with much reduced complexity.

REFERENCES

[1] T. Rappaport *et al.*, "Millimeter wave mobile communications for 5G cellular: It will work!" *IEEE Access*, vol. 1, pp. 335–349, May 2013.

[2] T. Bai and R. W. Heath, "Coverage and rate analysis for millimeter-wave cellular networks," *IEEE Trans. Wireless Commun.*, vol. 14, no. 2, pp. 1100–1114, Feb. 2015.

[3] T. Bai, R. Vaze, and R. W. Heath, "Analysis of blockage effects on urban cellular networks," *IEEE Trans. Wireless Commun.*, vol. 13, no. 9, pp. 5070–5083, Sept. 2014.

[4] W. Roh *et al.*, "Millimeter-wave beamforming as an enabling technology for 5G cellular communications: Theoretical feasibility and prototype results," *IEEE Commun. Mag.*, vol. 52, no. 2, pp. 106–113, Feb. 2014.

[5] Y. Niu, C. Gao, Y. Li, L. Su, and D. Jin, "Exploiting multi-hop relaying to overcome blockage in directional mmWave small cells," *J. Commun. Netw.*, vol. 18, no. 3, pp. 364–374, June 2016.

[6] S. M. Razavizadeh, M. Ahn, and I. Lee, "Three-dimensional beamforming: A new enabling technology for 5G wireless networks," *IEEE Signal Process. Mag.*, vol. 31, no. 6, pp. 94–101, Nov. 2014.

[7] W. Lee, S. R. Lee, H.-B. Kong, and I. Lee, "3D beamforming designs for single user MISO systems," in *Proc. IEEE GLOBECOM*, Dec. 2013, pp. 3914–3919.

[8] T. Bai, A. Alkhateeb, and R. Heath, "Coverage and capacity of millimeter-wave cellular networks," *IEEE Commun. Mag.*, vol. 52, no. 9, pp. 70–77, Sept. 2014.

[9] H. Elsawy, A. Sultan-Salem, M. S. Alouini, and M. Z. Win, "Modeling and analysis of cellular networks using stochastic geometry: A tutorial," *IEEE Commun. Surveys Tuts.*, vol. 19, no. 1, pp. 167–203, 2017.

[10] G. Giambene and V. A. Le, "Analysis of LTE-A heterogeneous networks with SIR-based cell association and stochastic geometry," *J. Commun. Netw.*, vol. 20, no. 2, pp. 129–143, Apr. 2018.

[11] M. D. Renzo, "Stochastic geometry modeling and analysis of multi-tier millimeter wave cellular networks," *IEEE Trans. Wireless Commun.*, vol. 14, no. 9, pp. 5038–5057, Sept. 2015.

[12] E. Turgut and M. C. Gursoy, "Coverage in heterogeneous downlink millimeter wave cellular networks," *IEEE Trans. Commun.*, vol. 65, no. 10, pp. 4463–4477, Oct. 2017.

[13] O. Onireti, A. Imran, and M. A. Imran, "Coverage, capacity, and energy efficiency analysis in the uplink of mmWave cellular networks," *IEEE Trans. Veh. Technol.*, vol. 67, no. 5, pp. 3982–3997, May 2018.

[14] S. Cen, X. Zhang, M. Lei, S. Fowler, and X. Dong, "Stochastic geometry modeling and energy efficiency analysis of millimeter wave cellular networks," *Wireless Netw.*, vol. 24, no. 7, pp. 2565–2578, Mar. 2017.

[15] *3GPP TR 36.814 V9.0*, "Further advancements for E-UTRA physical layer aspects," Tech. Rep. 2010.

[16] R. Hernandez Aquino, S. Zaidi, D. McLernon, M. Ghogho, and A. Imran, "Tilt angle optimization in two-tier cellular networks - a stochastic geometry approach," *IEEE Trans. Commun.*, vol. 63, no. 12, pp. 5162–5177, Dec. 2015.

[17] F. Baccelli and B. Blaszczyszyn, *Stochastic geometry and wireless networks, volume I and II*, Foundations and Trends in Networking: Vol. 4: No 1-2, pp 1-312. NoW Publishers, vol. 2. [Online]. Available: https://hal.inria.fr/inria-00403040,

[18] J. Andrews, F. Baccelli, and R. Ganti, "A tractable approach to coverage and rate in cellular networks," *IEEE Trans. Commun.*, vol. 59, no. 11, pp. 3122–3134, Nov. 2011.

[19] H. S. Dhillon, R. K. Ganti, F. Baccelli, and J. G. Andrews, "Modeling and analysis of K-tier downlink heterogeneous cellular networks," *IEEE J. Sel. Areas Commun.*, vol. 30, no. 3, pp. 550–560, Apr. 2012.

[20] M. Haenggi and R. K. Ganti, "Interference in large wireless networks," *Found. Trends Netw.*, vol. 3, no. 2, pp. 127–248, Feb. 2009.

[21] J. Wu, Y. Zhang, M. Zukerman, and E. K. N. Yung, "Energy-efficient base-stations sleep-mode techniques in green cellular networks: A survey," *IEEE Commun. Surveys Tuts.*, vol. 17, no. 2, pp. 803–826, 2015.

[22] S. Han, C. I, Z. Xu, and C. Rowell, "Large-scale antenna systems with hybrid analog and digital beamforming for millimeter wave 5G," *IEEE Commun. Mag.*, vol. 53, no. 1, pp. 186–194, Jan. 2015.

Mahdi Baianifar received his B.Sc. degree in Electrical Engineering from University of Zanjan, Iran and M.Sc. in Electrical Engineering from Sharif University of Technology, Tehran, Iran in 2011 and 2013, respectively. Currently, he is a Ph.D. student at Iran University of Science and Technology (IUST). His research interests are in the area of wireless communication systems and specially in the area of mmWave networks and application of the stochastic geometry in wireless communications.

S. Mohammad Razavizadeh received his B.Sc., M.Sc. and Ph.D. degrees in Electrical Engineering from Iran University of Science and Technology (IUST), Tehran, Iran, in 1997, 2000 and 2006, respectively. From 2005 to 2011, he was with Iran Telecomm. Research Center, as a Research Assistant Professor. Since 2011, he has been with the School of Electrical Engineering at IUST, where he is currently an Associate Professor and also head of the communications group. His research interests are mailnly in the area of signal processing for wireless communication systems. He is a Senior Member of the IEEE.

Hossein Akhlaghpasand received his B.Sc. degree in Communications Engineering from University of Zanjan, Zanjan, Iran, in 2012. He studied for his M.S. degree in Wireless Communication Networks at University of Tehran, Tehran, Iran, in 2012-2014. Currently, he is a Ph.D. student at Iran University of Science and Technology, and his research interests are in the area of wireless communication systems and multiple-antenna networks.

Inkyu Lee received the B.S. degree (Hons.) in Control and Instrumentation Engineering from Seoul National University, Seoul, South Korea, in 1990, and the M.S. and Ph.D. degrees in Electrical Engineering from Stanford University, Stanford, CA, USA, in 1992 and 1995, respectively. From 1995 to 2001, he was a Member of Technical Staff with Bell Laboratories, Lucent Technologies, where he studied high-speed wireless system designs. From 2001 to 2002, he was with Agere Systems, Murray Hill, NJ, USA, as a Distinguished Member of Technical Staff. Since 2002, he has been with Korea University, Seoul, where he is currently a Professor with the School of Electrical Engineering. In 2009, he was a Visiting Professor with the University of Southern California, Los Angeles, CA, USA. He has authored over 160 journal papers in the IEEE. He has 30 U.S. patents granted or pending. His research interests include digital communications, signal processing, and coding techniques applied for next generation wireless systems. He was elected a member of the National Academy of Engineering in Korea (NAEK) in 2015. He was a recipient of the IT Young Engineer Award at the IEEE/IEEK Joint Award in 2006, and the Best Paper Award at APCC in 2006, the IEEE VTC in 2009, and ISPACS 2013. He was also a recipient of the Best Research Award from the Korea Information and Communications Society in 2011, the Best Young Engineer Award from NAEK in 2013 and the Korea Engineering Award from National Research Foundation of Korea in 2017. He has served as an Associate Editor for the IEEE TRANSACTIONS ON COMMUNICATIONS from 2001 to 2011, the IEEE TRANSACTIONS ON WIRELESS COMMUNICATIONS from 2007 to 2011, the IEEE Wireless Communication Letters from 2011 to 2013, and the IEEE ACCESS from 2016 to 2017. He was the Chief Guest Editor of the IEEE JOURNAL ON SELECTED AREAS IN COMMUNICATIONS Special Issue on 4G Wireless Systems in 2006. He is an IEEE Fellow and an IEEE Distinguished Lecturer.